The evolution of polarization inside ultrathin PbTiO$_3$ films: a theoretical study

Y.B. Xue[a], D. Chen[a], Y.J. Wang[a], Y.L. Tang[a], Y.L. Zhu[a] & X.L. Ma[a]

[a] Shenyang National Laboratory for Materials Science, Institute of
Metal Research, Chinese Academy of Sciences, Wenhua Road 72,
110016 Shenyang, China
Published online: 16 Jun 2015.

PLEASE SCROLL DOWN FOR ARTICLE

Taylor & Francis
Taylor & Francis Group

The evolution of polarization inside ultrathin PbTiO₃ films: a theoretical study

Y.B. Xue, D. Chen*, Y.J. Wang, Y.L. Tang, Y.L. Zhu and X.L. Ma*

*Shenyang National Laboratory for Materials Science, Institute of Metal Research, Chinese
Academy of Sciences, Wenhua Road 72, 110016 Shenyang, China*

How to control the material properties by manipulating the unitcell thickness is crucial for applications of ferroelectric ultrathin films. To understand the polarization behaviour of ultrathin PbTiO₃ (PTO) films grown on SrTiO₃ (STO) substrate, we have systematically explored the strength and direction of polarization in each unitcell layer, using density functional theory combined with Born effective charge method. Strikingly, we find that the polar state of ultrathin PTO films is a composite result depending not only on thickness but also on boundary condition, initial polarization direction, etc. Besides, we also studied the surface effect on the polarization in the thicker PTO films for comparison with the ultrathin ones, which suggests that the surface effect is basically confined in a small range (3–5 unitcells thick at surface region) no matter what kinds of surface terminations and polarization directions.

Keywords: ultrathin films; first-principles calculation; polarization

1. Introduction

Ferroelectrics are a class of materials which display switchable macroscopic polarizations. They possess controllable polar states and electromechanical coupling, which makes them hold promise for extensive applications [1]. Especially ultrathin ferroelectric films have recently caught more and more people's interest due to the size reduction constraint imposed by the semiconductor industry [2].

At ultrathin thickness, experimental and theoretical works have lately confirmed the possibility of retaining the ferroelectric ground state, and even suggest the absence of a critical size in some ferroelectrics [3,4]. For instances, BaTiO₃ thin films between two metallic SrRuO₃ electrodes in short circuit condition lose their ferroelectric properties below a critical thickness of six unit cells (about 24 Å) [2]. Experimentally, it was shown that films below 50 Å display a significantly reduced polarization but still remain ferroelectric at room temperature [5].

Physical nature of ultrathin films has been found to be quite complicated, severely impacted by the chemical and local structural features as well as the defects [3,4,6,7]. However, little attention has been paid to the details such as the strength and direction inside each unitcell layer, which may have nontrivial relevance to the performance of

---

*Corresponding authors. Email: dchen@imr.ac.cn (D. Chen), xlma@imr.ac.cn (X.L. Ma)

the miniaturized devices. In this work, we choose PTO ultrathin film to study the evolution of polarization inside the ultrathin film under different conditions, motivated by the fact that PTO is one of the most important ferroelectric materials with the simple perovskite structure and extensive potential applications. Our results are expected to enrich one's knowledge of the properties of ultrathin ferroelectric films and help us engineer the desirable ferroelectric devices by manipulating the thickness, surface termination and initial polarization direction.

2. Methods

All calculations were carried out with the Vienna *Ab initio* Simulation Package [8,9] in the framework of density functional theory (DFT). We adopted the projector-augmented wave method [10,11] to describe the core-valence electron interaction and local density approximation was employed to treat the exchange correlation between electrons. The O: 2s and 2p, Ti: 3s, 3p, 3d and 4s, Sr: 4s, 4p and 5s, Pb: 5d 6s and 6p orbitals were chosen as valence states. The hard pseudopotential for O was adopted, and the plane-wave cut-off energy was set at 850 eV. The ions were relaxed until the maximum force on the atoms was smaller than 50 meV Å^{-1} and the total energy was obtained when it converged to 10^{-4} eV in the electronic self-consistent loop. Vacuum layer and dipole correction [12] were applied to avoid spurious interactions between periodic images. The Monkhorst–Pack [13] scheme was used for the *k*-point sampling and the Brillouin zone integration was performed with the Gaussian smearing method. Highly converged results were obtained utilizing $5 \times 5 \times 1$ *k*-point grid for both ultrathin PTO film and thicker PTO surface models.

As a benchmark test for our approach and parameterization, we first investigated the ground-state properties of the perfect bulk PbTiO$_3$ and SrTiO$_3$ (STO). A series of total energies were calculated as a function of the unit-cell volume and then fitted to the Murnaghan [14] equation of state. The optimized lattice parameters ($a = b = 3.864$ Å, $c = 4.051$ Å for PTO and $a = b = c = 3.862$ Å for STO) are very close to the experimental values ($a = b = 3.918$ Å, $c = 4.126$ Å for PTO [15] and $a = b = c = 3.905$ Å for STO [16]), so they can be safely adopted to build the film models.

The PTO/STO (0 0 1) film models were constructed with two in-plane sizes ($1a \times 1a$ and $\sqrt{2}a \times \sqrt{2}a$) and different thickness ranging from 1 unitcell layer to 10 unitcell layers. For every specific thickness, various surface terminations and initial polarization directions are considered and each model is represented by the symbols in the format: (initial polarization direction)_(PTO film thickness)_(surface termination). All of these models can be divided into four groups, such as up_*n*cell_PbO, up_*n*cell_-TiO$_2$, down_*n*cell_PbO and down_*n*cell_TiO$_2$. Figure 1(a) shows one of PTO ultrathin film models: *up_3cell_PbO*. The optimized cubic STO and tetragonal PTO unitcells are used as the building blocks for each supercell, but the in-plane lattice constants of the whole structure are constrained to the bulk cell parameters of STO and the concomitant strain relaxation of the ions are carried out under this constraint. Three STO unitcell layers in the bottom are fixed to simulate the bulk region, upon which two STO unitcell layers are allowed to relax corresponding to the interfacial part.

After full relaxations of PTO/STO (0 0 1) models, the polarization strength of each unitcell can be calculated by Born effective charge method [17]
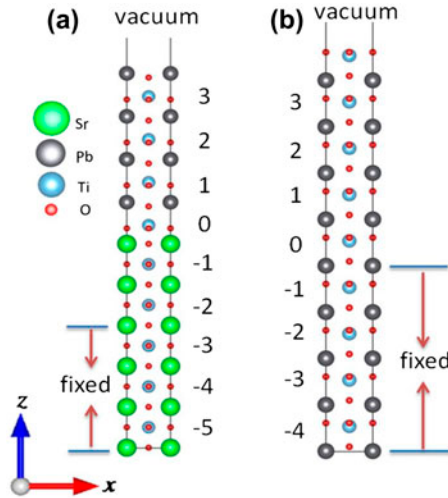
Figure 1. (colour online) Two examples of the calculated models used in the present work. (a) a PTO ultrathin film model: *up_3cell_PbO*; (b) a thicker PTO surface model: *down_3cell_TiO2* (details in §3.2). In Fig. 1, the number denotes the location of each unitcell and the fixed atoms correspond to the layers with the STO (or PTO) bulk properties.

$$P_i = \frac{e}{\Omega} \sum_{\alpha} \omega_{\alpha} Z_{\alpha}^* \cdot u_{\alpha}^{(i)} \tag{1}$$

where e is the electron charge, Ω is the volume of the five-atoms bulk unitcell, index α runs over all atoms of unitcell i, $u_{\alpha}^{(i)}$ is the displacement of atom α from its centrosymmetric position and ω_{α} is the weight factor. The Z_{α}^* is Born effective charge tensor, which is adopted from Ref. [18].

3. Results and discussion

3.1. Ferroelectric behaviour in ultrathin PTO/STO (0 0 1)

The computational results with the in-plane sizes of $1a \times 1a$ are summarized in Table 1. For each group, it is common that the ferroelectricity is suppressed when the film thickness is too thin. As Table 1 shows, the critical thickness is different for each group of models but within a range of 3–8 unitcells, which is quantitatively consistent with some previous conclusions that polarization can be obtained in ultrathin films with only several unitcells thickness [2,6]. Moreover, beyond each critical thickness, it is noteworthy that in each group the polarization direction undergoes a transition from *ab* plane to the normal direction of interface and we will discuss it in detail in next paragraph. It should be pointed out that the group of up_*n*cell_PbO only polarize on *ab* plane in the thickness range we studied here, but we believe that it would orient to *z* when films become thicker. The in-plane polar component was previously deduced in strained ultrathin PTO film via synchrotron X-ray diffraction [19]. In our work, the beginning of out-of-plane polarization was postponed compared with some other studies, but this is not a surprise, given that vacancies or 180° domains exist in previous studies [6,7] and the

Table 1. Calculated results of the polarization for each group of PTO/STO (0 0 1) ultrathin films with the in-plane sizes of $1a \times 1a$. The film thickness is measured by the number (n) of PTO unitcell layer. "No" means "no ferroelectricity", "ab" represents that the polarization direction is parallel to the (0 0 1) plane, and "up(down)" says that the polarization is parallel (anti-parallel) to the normal direction of the interface. The values are the average polarization strength (in unit of $\mu C/cm^2$).

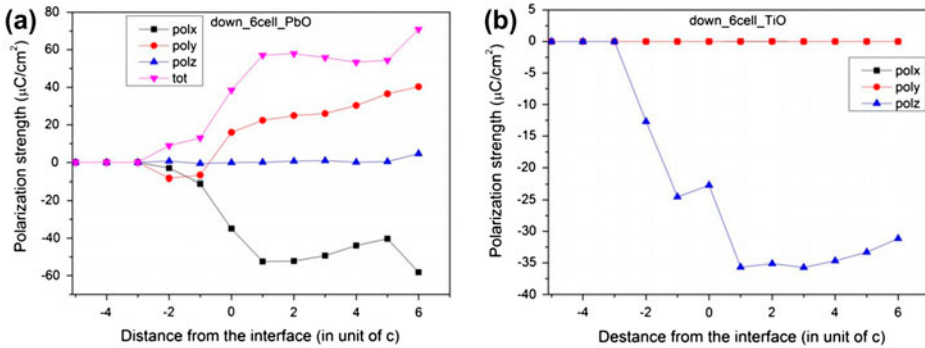| n	1	2	3	4	5	6	7	8	9	10
Up_$n$cell_PbO	No	No	No	No	No	No	No	*ab* 49.6	*ab* 52.0	*ab* 54.0
Up_$n$cell_TiO$_2$	No	No	No	No	No	No	*ab* 48.3	*ab* 46.8	Up 53.9	Up 58.6
Down_$n$cell_PbO	No	No	*ab* 47.9	*ab* 59.9	*ab* 52.5	*ab* 58.2	*ab* 56.5	Down 47.8	Down 58.8	Down 61.0
Down_$n$cell_TiO$_2$	No	No	*ab* 36.7	*ab* 51.0	*ab* 48.4	Down 34.3	Down 51.8	Down 58.4	Down 63.5	Down 67.7

Figure 2. (colour online) In the models (a) *down_6cell_PbO* with in-plane polarization (b) *down_6cell_TiO₂* with out-of-plane polarization, the *x*, *y* and *z* components of the polarization strength of each layer unitcell depend on its position (*a* distance from the interface).

results reported here have been obtained for a defect-free monodomain PTO films. At the beginning of ferroelectricity, it is also noteworthy that the average polarization strength of each model is almost as half as the spontaneous polarization value ($88.8 \, \mu C/cm^2$) of bulk PTO.

As mentioned above, a remarkable feature in Table 1 is that the polarization direction is in-plane first and then ends up with out-of-plane, which we may understand in terms of energy. If each model has the same surface termination, the increment of the system energy ΔE would be mainly divided into two parts

$$\Delta E \approx E_{dis} + E_{ele} \qquad (2)$$

where E_{dis} is the energy resulting from ionic displacement from the bulk equilibrium position and E_{ele} is the electrostatic energy due to the interaction between the polarization and the depolarization field. During the period of the pre-transition, the films are very thin and the depolarization field would be much strong if the out-of-plane polarization comes into being. So E_{ele} will be dominant in ΔE and the films would adopt the in-plane polarization so as to minimize it. When the thickness increases, however, the depolarization field would be weaker and the E_{dis} will become predominant, then it is preferable to form the bulk-like out-of-plane polarization.

In Figure 2, two representative models are given to exhibit how the polarization strength in each unitcell layer varies with its position (*a* distance from the interface). Figure 2(a) shows both the *x* and *y* components of the polarization in model *down_6cell_PbO* where nearly in-plane polarization takes shape, and Figure 2(b) only shows the *z* component of the polarization strength in model *down_6cell_TiO₂* where only the out-of-plane polarization evolved and the *x* and *y* components tend to zero. As we can see, *down_6cell_PbO* and *down_6cell_TiO₂* possess different polar state under the same thickness, which could confirms that the boundary condition is also one of the important influences.

At the same time, each group of films has its own features. As listed in Table 1, the average polarization strength is also concerned with the initial polarization direction: when the models are initially up-polarized, the critical thickness is comparatively larger

(7–8 unitcells), and when they are initially down-polarized, the critical thickness is reduced to 3 unitcells. Furthermore, when initial polarization is the same, TiO_2-terminated films seem to maintain stronger polarization than PbO-terminated ones. The cause might be the different work functions arising from the nonequivalent boundary conditions, which could lead to different depolarizing field, as pointed out in Ref. [3]. In addition, Figure 2 shows the induced polarization appears in STO substrate, and we find that initially down-polarized PTO films would produce stronger induced polarization in all of our models (not shown here). In our calculations, it is crucial to allow the internal coordinates of the STO interface to relax together with the PTO ions. For example, if all STO ions are fixed, the *down_7cell_TiO* will be relaxed to in-plane polarized state, not out-of-plane (not shown here). So the induced polarization in STO could play an important role in determining the ferroelectricity of PTO ultrathin films, as similarly reported before in $PbZr_{0.2}Ti_{0.8}O_3$–$SrTiO_3$ system [7].

Next, we explored the polarization behaviours of ultrathin PTO films using larger models, because the TiO_6 octahedra may have antiferro-distortive structures, especially when the films are very thin [6]. To incorporate this possible effect, the in-plane dimensions must be expanded at least to $\sqrt{2}a \times \sqrt{2}a$, corresponding to a $c(2 \times 2)$ in-plane unitcell. After the models were enlarged, the computations will become much more time-consuming. Table 2 lists the results of the films with the thickness less than 7 cell-layers. From Table 2, it is known that the thickness, surface termination and initial polarization direction, etc. are all the critical influences on the final states of ultrathin PTO films and the average polarization strength of most models is above the half of the spontaneous polarization value (88.8 $\mu C/cm^2$) of bulk PTO as the same as in the smaller models. Besides, the in-plane polarized states appear first, too. By contrasting with Table 1, a notable difference can be seen in the larger models: almost all the starting point of polarization has been brought forward. The polarized states could be even sustained down to 1 unitcell thickness in the groups of *down_ncell_PbO* and *down_ncell_TiO_2*. And like Tables 1 and 2 also exhibit that the polarization direction undergoes a transition from the in-plane to out-of-plane in the three groups (up_ncell_TiO_2, down_ncell_PbO, down_ncell_TiO_2).

In all of the larger models, the octahedral rotation was observed, which could not happen in the above smaller models due to the in-plane size limit. It was also found that different surface termination could lead to different levels of octahedral distortion. PbO surface layer could lead to more severe distortions than the TiO_2 counterpart, especially near the surface region, see Figure 3. The reasons may have something to do with the reconfiguration of the surface atoms. When the films are PbO terminated, the oxygen atoms move to two of the four surrounding Pb atoms to make their dangling bonds bonding again. However, when the films are TiO_2 terminated, the oxygen atoms in the uppermost PbO layer would not deviate much from the face centre sites due to the constraint from Ti atoms above them. Besides, the severe octahedral distortion causes also the stronger in-plane polarization, as we can see that in most cases the average polarization strength of in-plane polarization in the group of *down_ncell_PbO* is larger a bit than that in the group of *down_ncell_TiO_2*, refer to Table 2. Furthermore, after the in-plane sizes were expanded, in the group *down_ncell_PbO* and *down_ncell_TiO_2*, the strengths of in-plane polarized states are relatively constant, which may result from the fact that the depolarization field nearly have no effect on them. Let us look backwards to the previous $1a \times 1a$ systems, in the range where the out-of-plane polarization

Table 2. Calculated results of the polarization for each group of PTO/STO (0 0 1) ultrathin films with the in-plane sizes of $\sqrt{2}a \times \sqrt{2}a$. The meanings of the symbols and numbers below are the same as in Table 1.

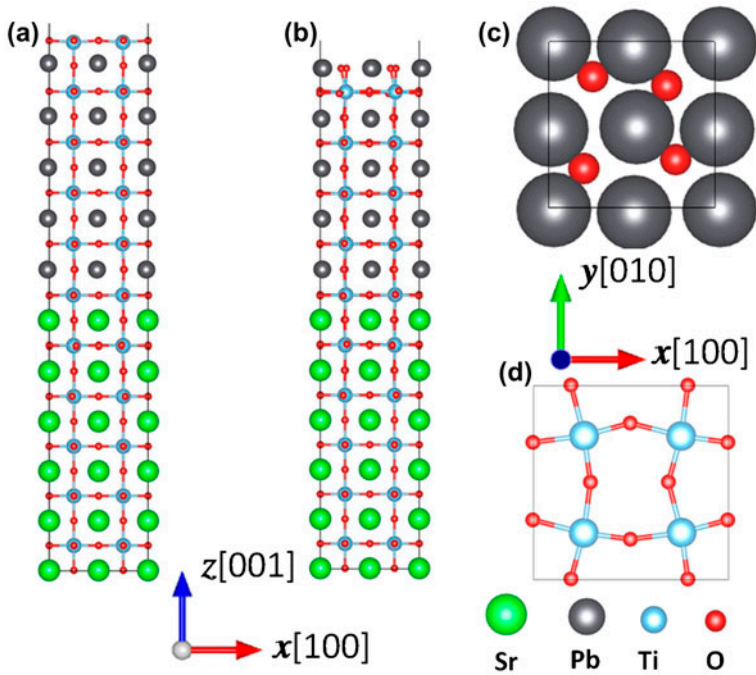| n	1	2	3	4	5	6	7	8	9	10
Up_$n$cell_PbO	No	No	No	No	ab 49.5	No	ab 53.5	ab 52.2	ab 57.2	ab 54.3
Up_$n$cell_TiO$_2$	No	No	ab 34.4	No	No	ab 49.9	No	ab 48.6	Up 53.7	Up 54.5
Down_$n$cell_PbO	ab 50.6	ab 52.6	ab 51.6	ab 52.5	ab 52.0	ab 52.4	ab 42.6	Down 47.4	Down 55.1	Down 62.2
Down_$n$cell_TiO$_2$	ab 39.5	ab 45.8	ab 46.6	ab 49.4	ab 49.1	ab 49.1	ab 50.1	Down 53.9	Down 62.8	Down 68.0

Figure 3. (colour online) Examples of the relaxed atomic structures after in-plane sizes were expanded (to be easier to understand, the in-plane sizes of the models shown here has been scaled up to $2a \times 2a$, based on the results of the models with in-plane sizes of $\sqrt{2}a \times \sqrt{2}a$). (a) *Down_4cell_TiO$_2$*; (b) *down_4cell_PbO*; (c) the uppermost PbO layer in *down_4cell_PbO*, where the oxygen atoms obviously deviate from the face centre sites and move to two of the surrounding Pb atoms; and (d) the uppermost TiO$_2$ layer in *down_4cell_PbO*, where the octahedral rotation can be seen apparently.

appears, the polarization strength become stronger and stronger gradually, for the depolarization field weakens as the film thickness becomes thicker. All of the above evidences suggest that the octahedral distortion could be one of the effective methods to eliminate or mitigate the adverse effects resulting from the depolarization field and make polarized states come into being in thinner PTO films.

Another characteristic of Table 2 is that in the series of *up_ncell_TiO$_2$* and *up_ncell_PbO*, the polar states are discontinuous with the thickness. Although *up_3cell_TiO$_2$*, *up_6cell_TiO$_2$* and *up_5cell_PbO* possess polar state, it was found that they underwent a nonpolarized state in the midway of relaxation and the energy difference between these two states is not too large, less than 10 meV/atom. So, we deduce that the octahedral distortion and the nonpolarized paraelectric state are two competitors in ultrathin PTO films.

It is also worth pointing out that there are only single-domain structures in our works, however, the multi-domain closure structures in PTO ultrathin films have been reported before [20]. The causes for the difference between theirs and ours may be due to the following factors. In the previous paper, the initial structures are 180° domains, which possibly lead to multi-domains after relaxation. And their models are very thin
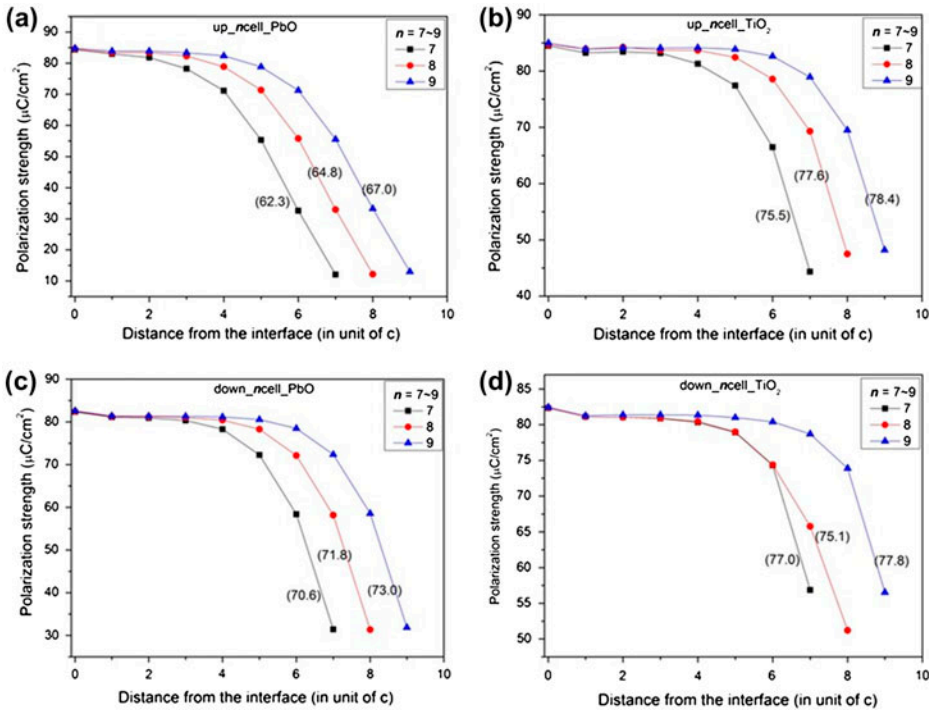
Figure 4. (colour online) Polarization strength of each unitcell layer varies with its position (*a* distance from the interface) in the four groups of models when the number (*n*) is respectively equal to 7, 8 and 9. The values in parenthesis are the average polarization strength in the PTO surface region (in unit of $\mu C/cm^2$).

(only 3 unitcells thick) free-standing PTO films, so, the depolarization field must be quite strong if single-domain exists. In their multi-domain closure structures, the in-plane polarization in some surface unit cells exists, which could weaken the polarization field. Moreover, because their models are free-standing, there are no other methods to screen the depolarization field, such as electrodes, ionic screening by substrate, and defects. [3,7].

From all above-mentioned, it is suggested that the polar state of PTO ultrathin films is closely related not only to the film thickness, but also to the boundary condition and the initial polarization direction, etc., of which one may make use to facilitate engineering of the desirable devices.

3.2. *Surface effect on the polarization in the thicker PTO films*

To make comparisons with the ultrathin films and further understand the surface effect on the properties of PTO films, thicker PTO films with in-plane sizes of $1a \times 1a$ are also calculated. For these models, there are no interfaces, and we just fixed the bottom 4 unitcells thick atomic layers to simulate the bulk part, allowing other ions to relax during calculation, see Figure 1(b) for a model example: *down_3cell_TiO$_2$*. Despite all this, we call the boundary in between fixed and unfixed ions "the interface" for the
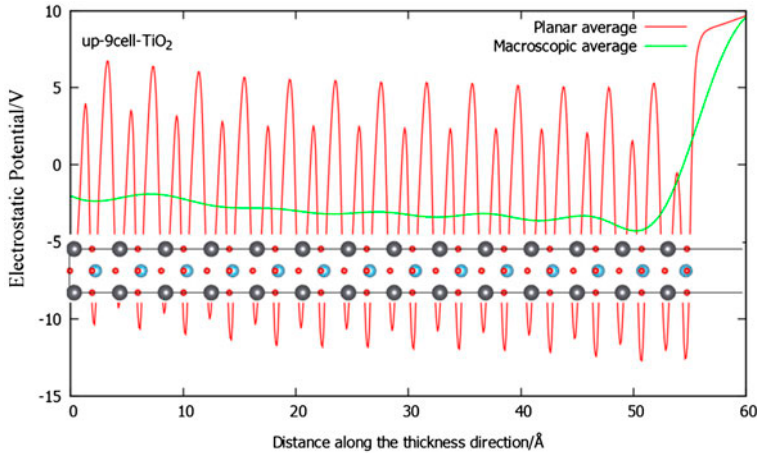
Figure 5. (colour online) The electrostatic potential for *up_9cell_TiO₂* surface model. The corresponding atomic structure has been put here to facilitate the understanding of the distance, in which the atoms are coloured according to type (Pb, grey; Ti, blue; O, red).

convenience of discussion. Similar to the case of ultrathin films, all of the models can also be divided into four groups.

Figure 4 shows the variation of the polarization strength in each unitcell layer with its position (*a* distance from the interface) for the four group models. In all of the four groups, when the layer is away from the surface and closer to the interface, the polarization strength will approach toward the value (88.8 μC/cm²) of bulk PTO. Although different kinds of surface terminations and initial polarization directions can lead to slight difference, the polarization strength decreases apparently only in a small region (3–5 unit-cells thick) near the surface; which suggests that the effect of surface may not play a critical role in the polarization of thicker PTO films. The distribution of electrostatic potential along the thickness direction was also studied and an example is given in Figure 5. It can be seen that the major fluctuation of macroscopic average potential occurs near the surface, consistent with the variation trend of the polarization.

4. Summary

Using DFT combined with Born effective charge method, the strength and direction of polarization in each unitcell layer are studied in ultrathin PTO films. It is found that the ferroelectricity will disappear if the film thickness is reduced to the critical thickness which is in a range of 3–8 unitcells. When the film thickness exceeds the critical value, the polarization direction undergoes a transition from the in-plane to out-of-plane, and the average polarization strength can persist at about half of the polarization value of bulk PTO. Above all, the polar state of ultrathin PTO films can be controlled by not only the film thickness, but also the boundary condition and polarization direction, etc., of which one may make use to facilitate engineering of the desirable devices. The in-plane polarization comes into being first and the average polarization strength of most models can persist above half of the polarization value of bulk PTO. In addition, it is

also observed that the octahedral distortion could make the polarized state stable in thinner PTO films. In addition, the surface effect on the polarization is also studied for the thicker $PbTiO_3$ films. No matter what kinds of surface terminations and polarization directions, the surface effect is basically confined in a small range (3–5 unitcells thick at surface region).

Acknowledgement

Disclosure statement

No potential conflict of interest was reported by the authors.

Funding

References

[1] J.F. Scott, Science 315 (2007) p.954.
[2] J. Junquera and P. Ghosez, Nature 422 (2003) p.506.
[3] N. Sai, A. Kolpak and A. Rappe, Phys. Rev. B 72 (2005) p.020101.
[4] N. Sai, C. Fennie and A. Demkov, Phys. Rev. Lett. 102 (2009) p.107601.
[5] C. Lichtensteiger, J.-M. Triscone, J. Junquera and P. Ghosez, Phys. Rev. Lett. 94 (2005) p.047603.
[6] D.D. Fong, G.B. Stephenson, S.K. Streiffer, J.A. Eastman, O. Auciello, P.H. Fuoss and C. Thompson, Science 304 (2004) p.1650.
[7] M.F. Chisholm, W. Luo, M.P. Oxley, S.T. Pantelides and H.N. Lee, Phys. Rev. Lett. 105 (2010) p.197602.
[8] G. Kresse and J. Furthmüller, Comput. Mater. Sci. 6 (1996) p.15.
[9] G. Kresse and J. Furthmüller, Phys. Rev. B 54 (1996) p.11169.
[10] P.E. Blöchl, Phys. Rev. B 50 (1994) p.17953.
[11] G. Kresse and D. Joubert, Phys. Rev. B 59 (1999) p.1758.
[12] L. Bengtsson, Phys. Rev. B 59 (1999) p.12301.
[13] H.J. Monkhorst and J.D. Pack, Phys. Rev. B 13 (1976) p.5188.
[14] F.D. Murnaghan, Proc. Nat. Acad. Sci. USA. 30 (1944) p.244.
[15] N. Takesue and H. Chen, J. Appl. Phys. 76 (1994) p.5856.
[16] A. Chen and Y. Zhi, J. Appl. Phys. 71 (1992) p.4451.
[17] B. Meyer and D. Vanderbilt, Phys. Rev. B 65 (2002) p.104111.
[18] W. Zhong, R.D. King-Smith and D. Vanderbilt, Phys. Rev. Lett. 72 (1994) p.3618.
[19] G. Catalan, A. Janssens, G. Rispens, S. Csiszar, O. Seeck, G. Rijnders, D. Blank and B. Noheda, Phys. Rev. Lett. 96 (2006) p.127602.
[20] T. Shimada, S. Tomoda and T. Kitamura, Phys. Rev. B 81 (2010) p.144116.